Numerical Study of Freestream Waves Induced Breakdown in Hypersonic Boundary Layer Transition

Jia Lei[1] and Xiaolin Zhong[2]
Mechanical and Aerospace Engineering Department, UCLA, Los Angeles, CA, 90095

As a continued effort in investigation of hypersonic boundary layer transition induced by fresstream waves, direct numerical simulations are performed on blunt cones over Mach 5.5 and Mach 6 flows. In this paper, a new approach is introduced to simulate the hypersonic flow over blunt cone from laminar to the breakdown stage in transition. The disturbance waves are introduced into freestream instead of generating within the boundary layer. The new approach breaks the direct numerical simulation into three parts: mean flow computation, linear receptivity simulation and nonlinear breakdown simulation. With this approach, it is possible to directly link the freestream receptivity process to the final breakdown stage so that the complete transition process can be better understood. The ultimate goal is to develop a robust numerical tool to carry out hypersonic boundary layer flow simulation over blunt cone to the non-linear breakdown stage and use it for future transition studies.

Nomenclature

a	=	non-dimensional wave speed
e	=	total energy per unit volume
Fi	=	inviscid flux vector
Fv	=	viscous flux vector
F	=	frequency
M	=	Mach number
Pr	=	Prandtl number
P	=	pressure
R_n	=	nose radius
Re	=	Reynolds number
Re_n	=	Reynolds number based on the nose radius
s	=	distance along the cone surface from the nose tip
T	=	temperature
u, v, w	=	velocity components
ξ, η, ς	=	local curve-linear coordinates
y_n	=	local normal distance from cone surface
α	=	streamwise wave number
ω	=	angular frequency
μ	=	viscosity
ρ	=	density
τ	=	shear stress
Superscript *	=	dimensional quantity
Subscript ∞	=	freestream quantity

[1] Graduate Student Researcher, MAE Department, UCLA, and AIAA Student Member. jxlei@ucla.edu
[2] Professor, MAE Department, UCLA, and AIAA Associate Fellow. xiaolin@seas.ucla.edu

I. Introduction

The prediction of laminar-turbulent transition of hypersonic boundary layers is critically important to the development of hypersonic vehicles that are to be used for rapid global access[1]. Boundary layer transition has first-order impacts on aerodynamic heating, as well as drag and control of hypersonic vehicles. Extreme heat transfer rates are arguably the prime constraint in the design of hypersonic aircraft. Some success has been obtained in predicting heating rates in fully laminar or fully turbulent flow, but accurate predictions in a transitional regime remain elusive. Uncertainty in heat transfer rate requires large factors of safety to be used in current vehicle designs. Improved computational accuracy could lead to significant improvements in hypersonic vehicle performance by allowing the removal of unnecessary weight in the thermal protection system.

The success of transition and related heating prediction relies on the good understanding of the relevant physical mechanisms leading to transition. In spite of considerable efforts in experimental, theoretical, and numerical studies, many critical physical mechanisms underlying hypersonic boundary-layer transition are still poorly understood. Engineering design of hypersonic vehicles has mainly been based on transition criteria obtained by empirical correlations of experimental data. The e^n method, which predicts boundary layer transition based on normal-mode linear stability theory, is by far the most successful mechanism-based prediction method for transition prediction. Nevertheless, the e^n method suffers from a major drawback that it does not consider the effects of receptivity of the boundary layer to freestream disturbances, surface roughness, or other perturbation sources. In reality, the transition location is very sensitive to the level of forcing disturbances[2]. Furthermore, the e^n method does not apply in the case of bypass transition.

Because of the difficulties in conducting hypersonic experiments and the complexity of hypersonic flows, fundamental hypersonic studies will increasingly rely on the use of direct numerical simulations (DNS). In order for a DNS technique to perform reliable "numerical experiments", it is necessary to develop and validate high-order accurate numerical algorithms suitable for highly accurate simulation of transient high-speed flows. So far, our group at UCLA have developed and validated our own fifth and higher order DNS methods and computer codes for the DNS studies of hypersonic boundary layer stability and transition over non-trivial geometries with bow shock effects[3-6]. We have done many studies on the receptivity and stability of a number of 2-D and 3-D hypersonic flows over blunt bodies and flat plates[7-15]. The uniqueness and the advantage of our numerical approach is to use our new high-order shock fitting schemes to accurately account for the effects of bow shock interaction and the effects of entropy layer in simulation of 3-D Navier-Stokes equations in hypersonic boundary layer receptivity and stability. These numerical simulations have led to a better understanding of hypersonic boundary layer receptivity and stability physics.

Due to the enormous requirement on computer times and on computer memory, DNS studies on boundary layer transition have been limited to idealized cases of boundary layer response to imposed forcing waves. So far, the complete process of laminar-turbulent transition from leading edge to the beginning of transition has not been computed by direct numerical simulation. Such a task has been commonly regarded as beyond the capability, in terms of computer times and memory, of currently available computers. On the other hand, if possible, such simulation can have significant impact on the state of the art in transition prediction because the effects of freestream noise on transition location can be predicted by DNS. We believe that with our proposed simulation method and the availability of large scale parallel computation power, we can tackle the problem of DNS of hypersonic boundary layer transition.

Therefore, the purpose of this paper is to develop, demonstrate, and validate a robust and reliable DNS computational tool for the numerical simulation of the complete process of hypersonic boundary layer transition. Such simulation tool can be valuable in the prediction of surface heat transfer rates in transitional hypersonic boundary layers. Our main idea is to use DNS to compute the complete transition process under realistic freestream noise and disturbances by dividing it into a three step process.

Since 1990s, significant progress has been made by several research groups in DNS studies of fundamental mechanisms leading to nonlinear breakdown and transition of supersonic and hypersonic boundary layers [16-18]. In DNS studies, the full 3-D nonlinear Navier-Stokes equations are computed to simulate the development and nonlinear interaction of the disturbances waves. A number of transition mechanisms have been identified and

studied. In some cases, transition was simulated up to the beginning of turbulence. Detailed information on the formation and evolution of transitional flow structures, as well as average heating rates and skin friction, could be obtained by the simulation. It was found that the transition mechanisms for supersonic boundary layers include secondary instability of either sub-harmonic or fundamental resonances [19]. By using DNS, Thumm [20] and Fasel et al. [21] discovered a new breakdown mechanism for a boundary layer at Mach 1.6, which they termed oblique breakdown. This breakdown to turbulence is initiated by the nonlinear wave interaction of two oblique instability waves with equal but opposite wave angles. The mechanisms have also been confirmed by many researchers, including Chang and Malik [22]. For supersonic flows, it was shown that oblique breakdown leads to a more rapid transition than the secondary instability mechanisms. It also requires much lower threshold disturbance amplitudes for the nonlinear development [23]. For these reasons, oblique breakdown has been suggested to be of practical importance for supersonic transition in low-disturbance environments [24, 25].

Husmeier and Fasel [26] did DNS studies of secondary instability mechanisms of hypersonic boundary layers over cones with a circular cross section. The computational domain is a cut-out section of the whole flow field (*Fig.1*). Though hypersonic boundary layer is most unstable to second-mode two-dimensional waves, their investigations indicated that secondary instability mechanisms involving two-dimensional waves appear to be of lesser importance in the nonlinear stages of breakdown. Instead, second-mode oblique waves at small wave angles, which are almost as amplified as second-mode two-dimensional waves, were found to dominate the nonlinear behavior. It seems that further studies are necessary in order to confirm this conclusions because extensive experimental results have pointed to the dominant of 2-D second mode before transition in hypersonic boundary layers [27, 28].

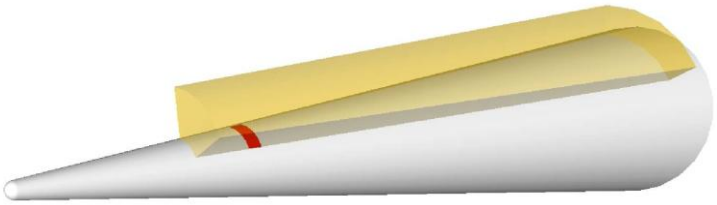

Fig.1. Computational domain used in Husmeier and Fasel's DNS simulation [26].

For hypersonic boundary layer transition, Pruett and his colleges did spatial DNS of hypersonic boundary layers of Mach 8 flow over a cone of eight-degree half angle [16, 17, 29]. The transitional state was triggered by a symmetric pair of oblique second-mode disturbances whose nonlinear interactions generate strong streamwise vorticity, which leads severe spanwise variations in the flow and eventual laminar breakdown. In their simulations, the PSE method was used to compute the weakly and moderately nonlinear initial stages of the transition process and, thereby, to derive a harmonically rich inflow condition for the DNS. The strongly nonlinear and laminar-breakdown stages of transition were subsequently computed by well-resolved DNS.

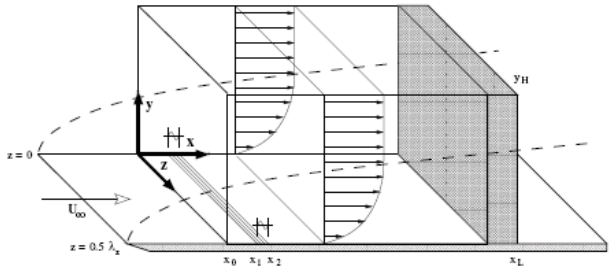

Fig.2. A typical DNS simulation domain on a flat–plate boundary layer.

However, most of the previous DNS research of compressible boundary layers has been mainly focused on supersonic flow of Mach less than 5 and on simplified flow over flat plates (*Fig.2*). In addition, the simulation was not related to practical flows because only theoretical or artificial forcing waves were used to study transition

mechanisms. To date, with the exception of Rai and Moin [30], virtually all of the numerical experiments have simulated controlled rather than natural occurring instability processes. In a controlled experiment, instability waves of a particular wavelength (temporal) or frequency (spatial) are excited by imposed forcing. In contrast, in natural transition, the input is random, and the flow itself selects the preferred instability modes. A few of the cited simulations are hybrid in the sense that the primary instability wave is imposed, whereas secondary instability is triggered by low-level noise [31, 32].

Receptivity of low-speed incompressible boundary-layer flows has been extensively studied in the last three decades[2]. However, there have been only a limited number of theoretical[33-38] and computational[7-15, 39] studies on the receptivity of compressible boundary layers. Fedorov et al.[33-36, 40] showed that the receptivity mechanisms of supersonic and hypersonic boundary-layer flows are essentially different from those of subsonic and relatively low supersonic flows. Specifically, they found that two boundary-layer wave modes, which were termed Mode 1 and 2, can be synchronized with the fast and slow acoustic waves in the leading edge region, respectively. Secondly, Mode 1 can be synchronized with external entropy/vorticity waves with a phase speed equal to free-stream velocity. Third, there is a synchronization point between Mode 1 and 2 near the Branch I of the second-mode neutral stability point.

The main features of the supersonic boundary-layer normal modes analyzed by Fedorov et al. were in qualitative agreement with Zhong's numerical simulation[7, 8, 10]. We showed that both Mode I and the first Mack mode can convert to the unstable second Mack mode in numerical simulations. It was shown that the receptivity leads to the excitation of both Mack modes and a family of stable modes, i.e., mode I, mode II, etc. The forcing fast acoustic waves do not interact directly with the unstable second Mack mode. Instead, the stable mode I waves interact with both the fast acoustic waves near the leading edge and the unstable Mack-mode waves downstream. Through this two-step interaction process, the stable mode I waves transfer wave energy from the forcing fast acoustic waves to the second Mack-mode waves inside the boundary layer. These receptivity studies have led to a better understanding of the hypersonic boundary receptivity mechanisms for instability modes. The receptivity results can be coupled with a nonlinear breakdown in the DNS of hypersonic boundary layer transition.

The objective of the paper is to perform a direct numerical simulation with natural disturbance spectrum coming from the freestream. The simulation will be carried out to reach the non-linear breakdown stage in transition. It is expected that the success of this DNS will help in understanding the flow structure and instability mechanisms during the non-linear breakdown process. Also, once the approach is proved successful, it will provide a reliable tool in predicting the transition in hypersonic boundary layer.

II. Numerical Method and Solution Strategy

A. Governing Equations

The governing equations are the unsteady compressible 3D Navier-Stokes equations, which can be written in the following conservative form:

$$\frac{\partial U^*}{\partial t^*} + \frac{\partial F_j^*}{\partial x_j^*} + \frac{\partial F_{vj}^*}{\partial x_j^*} = 0 \tag{1}$$

where $U^* = (\rho^*, \rho^* u_1^*, \rho^* u_2^*, \rho^* u_3^*, e^*)$, and superscript "*" represents dimensional variables. The F^* s are invicid and viscous flux terms that can be expanded as

$$F^*_j = \begin{Bmatrix} \rho u_j \\ \rho u_{j1} u_j + p\delta_{1j} \\ \rho u_{j2} u_j + p\delta_{1j} \\ \rho u_{j3} u_j + p\delta_{1j} \\ (e+p)u_j \end{Bmatrix} \quad \text{and} \quad F^*_{vj} = \begin{Bmatrix} 0 \\ \tau_{1j} \\ \tau_{2j} \\ \tau_{3j} \\ \tau_{jk} u_k - q_j \end{Bmatrix} \tag{2}$$

The Cartesian coordinates are denoted by (x_1^*, x_2^*, x_3^*) in tensor notation. In the current simulation of axisymmetric flow over blunt cones, x^* is the coordinate along the centerline of the cone pointing toward the downstream direction. The origin of coordinate is co-located with the center of spherical nose.

B. Numerical Scheme

A High-order shock-fitting code originally developed by Zhong [4] is used to compute the flow field bounded by the bow shock and cone surface. The flow variables behind the shock are determined by Rakine-Hugoniot relations across the shock and the characteristic compatibility equations. Since the performance of the linear stability analysis is very sensitive to the base flow solution, the base flow must be very accurate in order to obtain the reliable results on the linear stability analysis. The shock-fitting scheme had been tested and proven accurate and reliable by different test case.

C. Solution Strategy

We propose to tackle this problem by using our innovative approach of separating the linear receptivity simulation from the nonlinear breakdown simulation. In this way, we are able to make the computational cost manageable by breaking the whole simulation process into 3 major steps:

- **Step I: Mean Flow Simulation**. The high accuracy mean flow solution without any freestream disturbance is obtained using our high-order shock-fitting code. This is done with multiple zone procedure by cutting the whole computational zone along the cone surface into shorter subzones and marching the solution downstream as long as we needed.

- **Step II**: **Linear Receptivity Simulation.** In step two, a series of linear receptivity simulations are carried out with different types of freestream disturbances: fast acoustic wave, slow acoustic wave and entropy wave. They are imposed in the receptivity simulation to the mean flow solution in the freestream. In the receptivity simulation of each type of disturbance, multiple frequencies are imposed to better represent the freestream wave spectrum. The receptivity simulation will be carried all the way to the end of the linear growth region. This location can be estimated by LST analysis or by investigation of simulation result. The linear receptivity simulation is computationally much less expensive than the full scale 3D non-linear simulation due to the fact that the simulation is axis-symmetric in nature. So, a 2D simulation with significant less number of grid points is sufficient.

- **Step III**: **Non-linear Breakdown Simulation**. After finishing the receptivity simulation, the entrance condition for the 3D non-linear simulation can be constructed based on the solutions obtained from the linear simulation. The inflow boundary condition is obtained from the preceding linear receptivity simulations. Fourier decomposition is applied to separate disturbance waves into different frequencies. Therefore the inflow disturbance can be from freestream fast/slow acoustic wave, entropy waves and combination of all. In this paper, we only focus on using the disturbance profile from freestream fast acoustic waves for code testing purpose. A more realistic disturbance profile can be constructed to be consistent with those from typical experiments. Since the Fourier decomposition in time can be applied to separate the solution in linear region for different frequencies, we can rescale the magnitude

of solution for each specified frequency to match the freestream noise spectrum in a typical experiment. Therefore, the complete transition process due to different freestream noise profile can be simulated by using the receptivity results. So that, we just need to do the receptivity simulation once for different cases of different freestream spectra and different noise amplitudes. We can simply rescale the magnitude of each frequency to match the freestream value in the spectrum. As a result, for various freestream disturbance profiles, only step three is repeated to investigate the effects of freestream noise levels on the location of boundary layer transition.

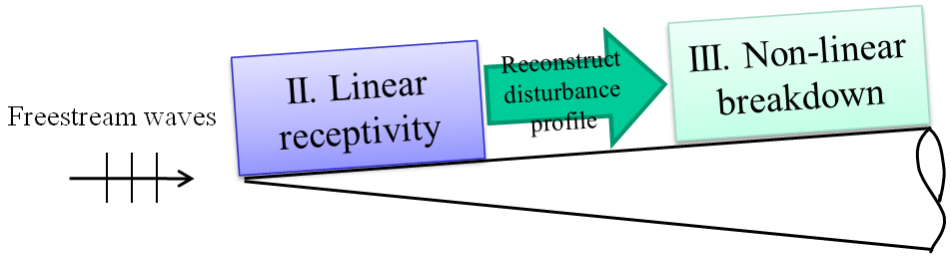

Fig. 3. Schematic of proposed simulation procedures to non-linear breakdown

III. Computation Setup

A. Flow Conditions for Mach 5.5 Test Case

In this paper, we used Stetson's Mach 5.5 test case [41] for code testing purpose, because the linear receptivity process of this case has been thoroughly studied in our previous papers. The specific flow conditions are:

- $M_\infty = 5.468$
- $P_\infty^* = 7756.56\,Pa$, $T_\infty^* = 174.46K$
- Wall temperature: $T_w = 296K$
- $\gamma = 1.4$, $\mathrm{Pr} = 0.72$, $R^* = 286.94 Nm/kgK$
- Freestream unit Reynolds number: $\mathrm{Re}_\infty^* = 18.95\times10^6\, m^{-1}$
- Blunt cone half angle: $\theta = 8^\circ$, the freestream flow has a zero angle of attack
- Parameters in Sutherland's viscosity law: $T_r^* = 288K$, $T_s^* = 110.33K$, $\mu_r^* = 0.17894\times10^{-4}\, kg/ms$

We have already obtained the mean flow solutions and the freestream linear receptivity results for cones with three different nose radii in previous study. In this paper, we will show the non-linear breakdown simulation on the case with nose radius of 0.156 inch to demonstrate the capability of our simulation program.

B. Flow Conditions of TAMU Mach 6 Study Case

In the effort to collaborate with Hypersonic Transition Research Center, we will continue our numerical study using the flow conditions and cone models that the experimental team at TAMU used to develop their Mach 6 quiet

tunnel, such that the experiment and simulation effort can assist each other on their way of making better understanding of the hypersonic transition process. The detail flow conditions are listed below.

- $M_\infty = 5.91$
- $P_\infty^* = 622.84\,Pa$, $T_\infty^* = 56.35K$
- Wall temperature: $T_w =$ adibatic wall
- $\gamma = 1.4$, $\Pr = 0.72$, $R^* = 286.94 Nm/kgK$
- Freestream unit Reynolds number: $\mathrm{Re}_\infty^* = 9.25\times10^6\, m^{-1}$
- Blunt cone half angle: $\theta = 5^\circ$, the freestream flow has a zero angle of attack
- Parameters in Sutherland's viscosity law: $T_r^* = 288K$, $T_s^* = 110.33K$,

$$\mu_r^* = 0.17894\times10^{-4}\, kg/ms$$

Using the cone geometry provided by TAMU tunnel experiment team, we have already obtained the mean flow solutions for cones with three different nose radii in previous study. In this paper, we will carry out the non-linear breakdown simulation placing the focus on the case with nose radius of 0.125 inch.

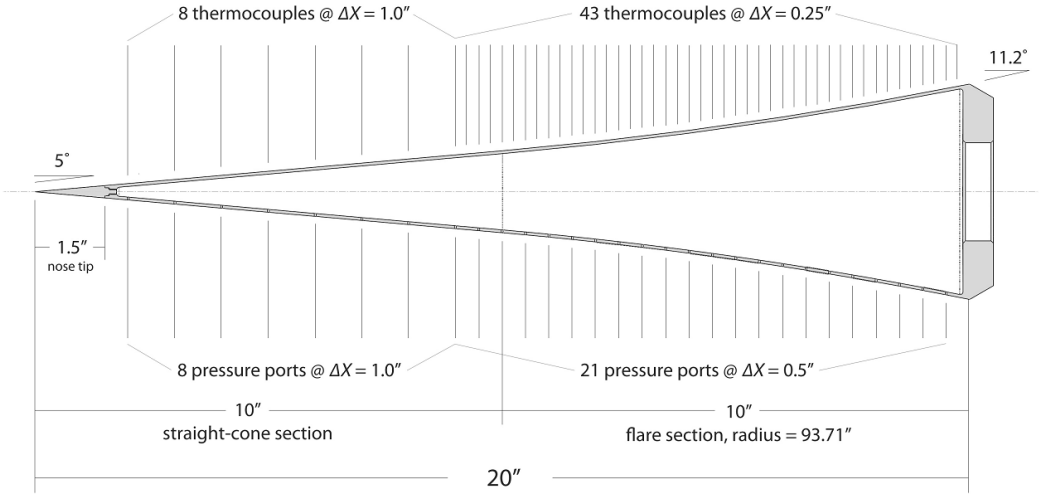

Fig. 4. Schematic of Cone Geometry.

C. Sponge Layer at the Exit of Nonlinear Breakdown Simulation

For the nonlinear portion of the unsteady simulation, a sponge layer needs to be added to the outflow to avoid spurious reflection and blowing up. In the sponge layer, an additional term is used to force the solution toward target values as shown in eq. (3). U is the place holder for any conservative variable. $A(\xi)$ is a weight function smoothly increases from 0 to 1. The steady flow values are used as the reference values in the equation, so that the flow will be forced back to laminar state.

$$\left(\frac{dU}{dt}\right)_{adj} = \frac{dU}{dt} - \sigma A(\xi)\left[U - U_{ref}\right] \tag{3}$$

$$A(\xi) = \frac{1}{t_{ref}} e^{-\xi^4/10}(1-\xi^{50})^4 \tag{4}$$

$$t_{ref} = \frac{u_\infty}{L_{buf}} \tag{5}$$

$$\xi = \frac{x_L - x}{L_{buf}} \quad (1 \geq \xi \geq 0) \tag{6}$$

D. Freestream Pulse Model for TAMU Mach 6 Case

For the numerical study of the TAMU Mach 6 case, we want to exam the linear receptivity response of freestream waves for a wide range of frequencies. In order to do so, we introduce a Gaussian pulse into the freestream that contains a continue frequency spectrum. Depending on the type of disturbance, The Gaussian pulse can be applied to acoustic wave, entropy wave and vorticity wave as well. The formula of the pulse is the following:

$$q(x,t) = q_0 \exp\left(-\frac{\left(X_0 - ut\right)^2}{\sigma^2}\right) \tag{7}$$

In eq.(3), σ is the parameter dictates the band width of the Gaussian pulse. u is the pulse transport velocity which varies to the type of disturbance. For the case of fast acoustic pulse, u equals to $(u_\infty + a)$. Fig. 5 shows the pulse as function of time for $\sigma = 0.0005$ and its frequency spectrum assuming unity wave amplitude. This is the same pulse model we used on our TAMU Mach 6 case freestream receptivity simulation.

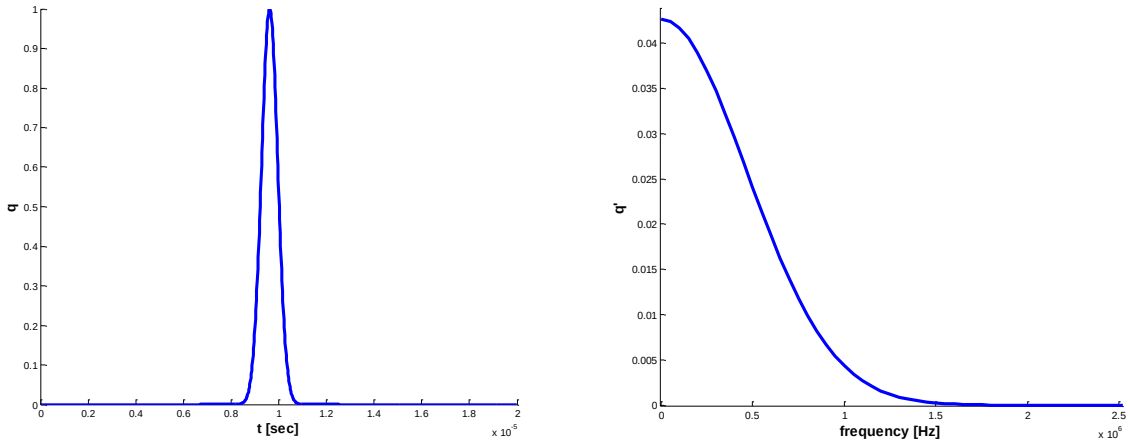

Fig. 5. Gaussian pulse function used for freestream fast acoustic wave and its frequency spectrum.

IV. Nonlinear Breakdown Simulation of Mach 5.5 Case

In this paper, we first use Stetson's Mach 5.5 test case[41] for code testing purpose. We have already obtained the mean flow solution in previous linear stability study [42]. Also, the linear receptivity simulations for both slow and fast acoustic waves have been completed. In this paper, we will carry out the non-linear breakdown simulation with the focus on the case of nose radius of 0.156 inch.

As the first trial on testing the capability of current simulation code, we used only the fast acoustic wave receptivity result at the inlet of simulation domain. The receptivity result included 15 discrete wave frequencies uniformly distributed between 52.55 kHz and 788.26 kHz. To investigate the non-linear growth effect to the unsteady simulation, the amplitude level at the inlet of computation domain is scaled up from the original linear receptivity simulation to shorten the linear growth region. The disturbance level at the entrance is scaled up to equivalent to impose the disturbance of 0.5% of the freesteam value from the leading edge. Waves contained 15 frequencies are imposed at the inlet of the computation domain. In addition, to enrich the spanwise wave spectrum to mimic the true three dimensional case, some small magnitude random noise were applied on top of the two dimensional primary waves. The max amplitude of random noise was set to be 5% of instantaneous primary wave amplitude. In Fig. 6, the pressure disturbance contour on the surface of cone body is shown. It can be clearly seen that, the waves are dominantly two dimensional at the area close to the inlet. Immediately, it entered the linear growth region between x=0.6 and 0.7 m. After x=0.75 m, the disturbance reached the saturation level and started to decrease a bit. The breakdown process started at around x=0.82 m.

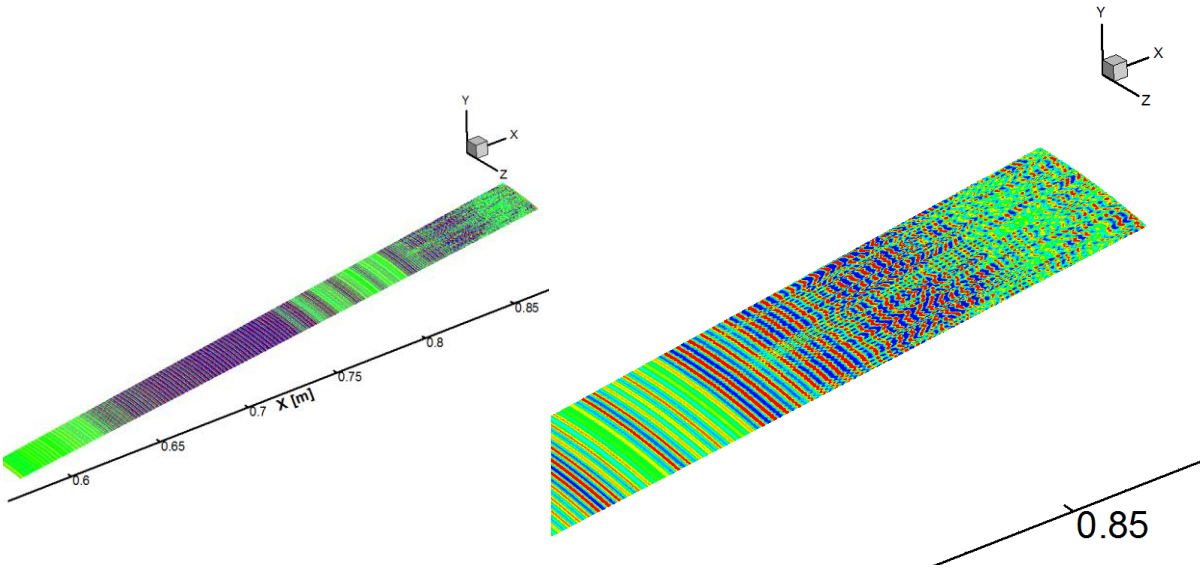

Fig. 6. Pressure disturbance (top view) on the surface and the blow-up view of the breakdown region.

Fig. 7 shows the evolution of spanwise vorticity near the wall. A clear "rope-like" vorticity wave pattern was observed. Fig. 8 shows the development of streamwise vorticity in the breakdown region. At the early breakdown region, the streamwise vorticity waves are very weak and two dimensional. As they progress further downstream, the three dimensional feature appeared and the vorticity waves tended to break down to smaller and smaller scales.

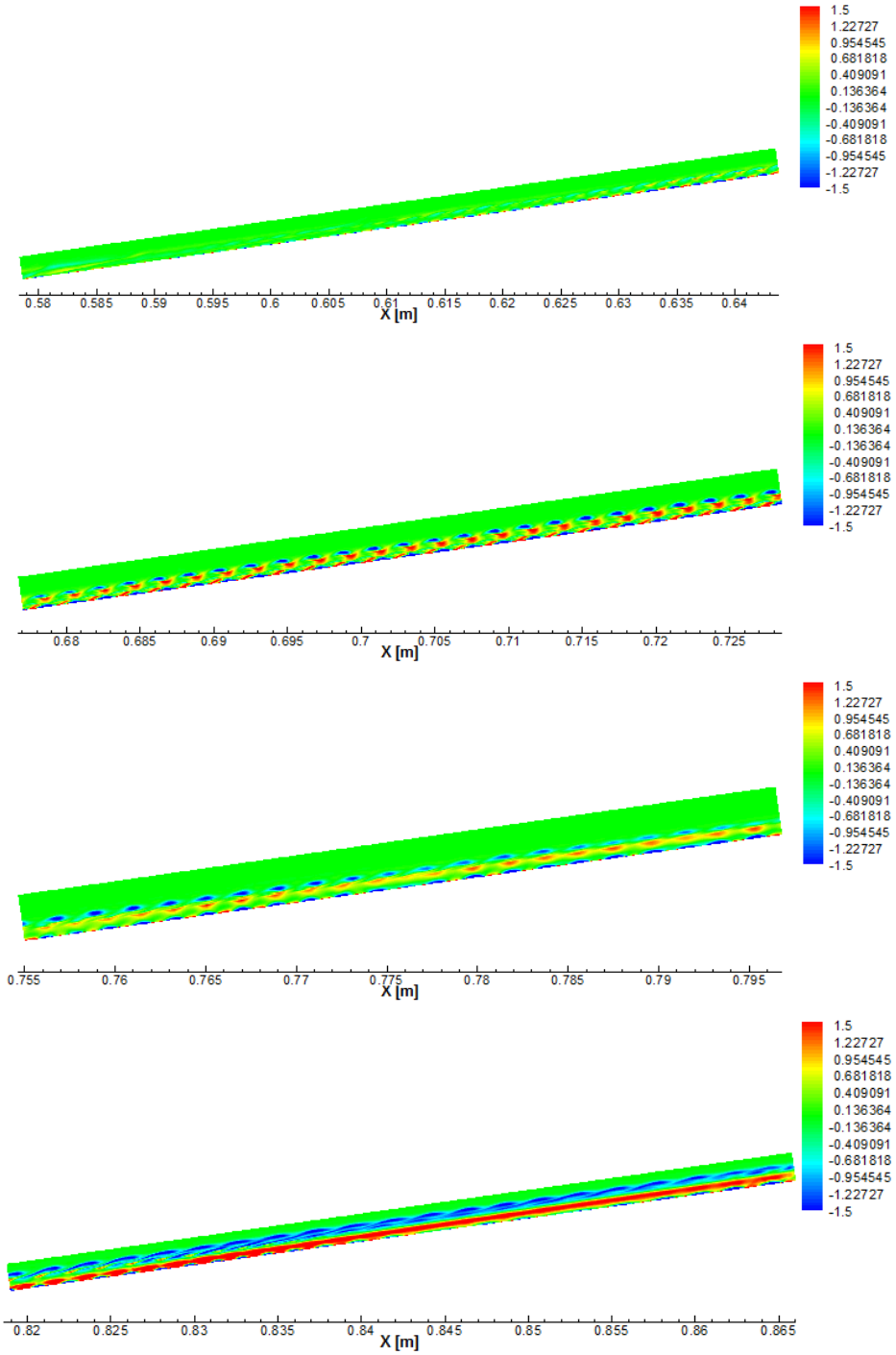

Fig. 7. Spanwise vorticity contours (side view) on the symmetric plane of cone.

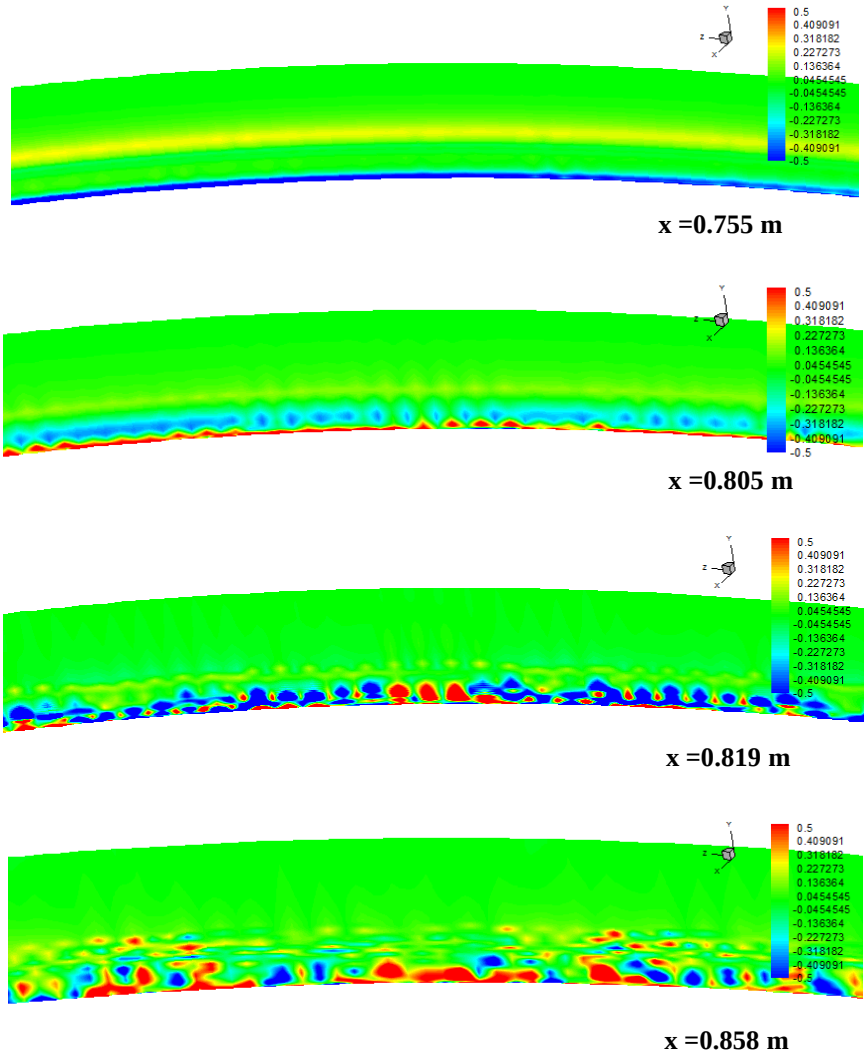

Fig. 8. Streamwise vorticity contours (cross-section view) at different streamwise locations.

From our previous LST analysis [43], we predicted the dominant second mode unstable frequency in the current simulated region is from 600 to 700 KHz. The LST N factor result is provided in Fig. 9. After the FFT decomposition of current result, we can identify the wave amplitudes for each frequency and spanwise wave number so that we are able to track the evolution of each wave mode. Fig. 10, Fig. 11and Fig. 12 show the disturbance frequency spectrum for selected spanwise wave numbers. At spanwise wave number k=0, the spectrum represents the two dimensional disturbance waves which are the primary waves from the receptivity simulation. The 2D waves between 500 kHz and 750 kHz amplified more than one order of magnitude within the linear growth region which is qualitatively matched with the LST analysis. However, after their amplitude reach their max values. They tended to decay quickly. On the other hand, the non-zero spanwise wave number behaved quiet differently. The non-zero spanwise waves represent the random noise that was added at the inlet. They are very weak initially and decayed during the linear growth region. Nonetheless, when the 2D primary waves reached saturation, they started to amplify. Also, the waves at higher spanwise wave number grow slight faster and earlier than the ones at lower spanwise wave number.

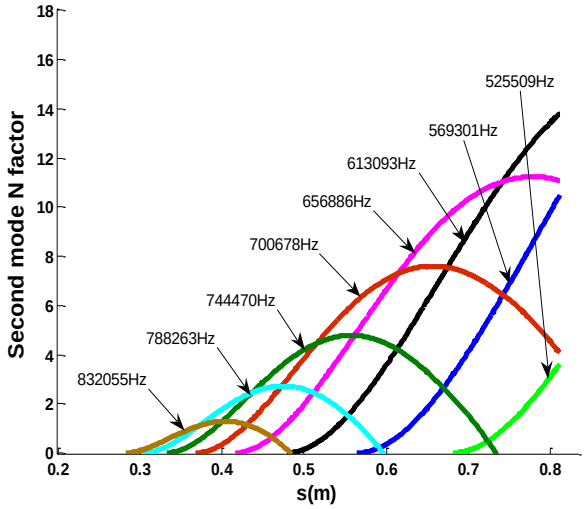

Fig. 9. Linear Stability (LST) N factor for the Stetson's Mach 5.5 case with 0.156 inch nose[43].

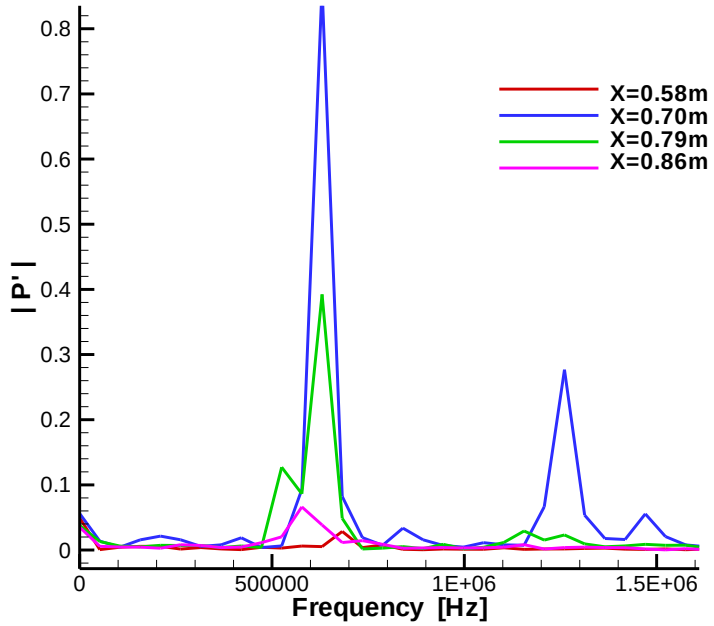

Fig. 10. Pressure amplitudes spectrum for spanwise wave number k=0

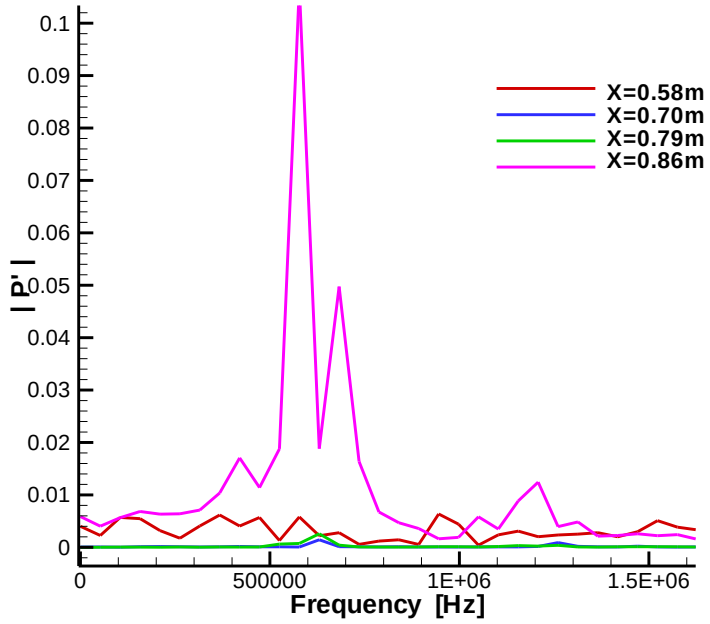

Fig. 11. Pressure amplitudes spectrum for spanwise wave number k=480

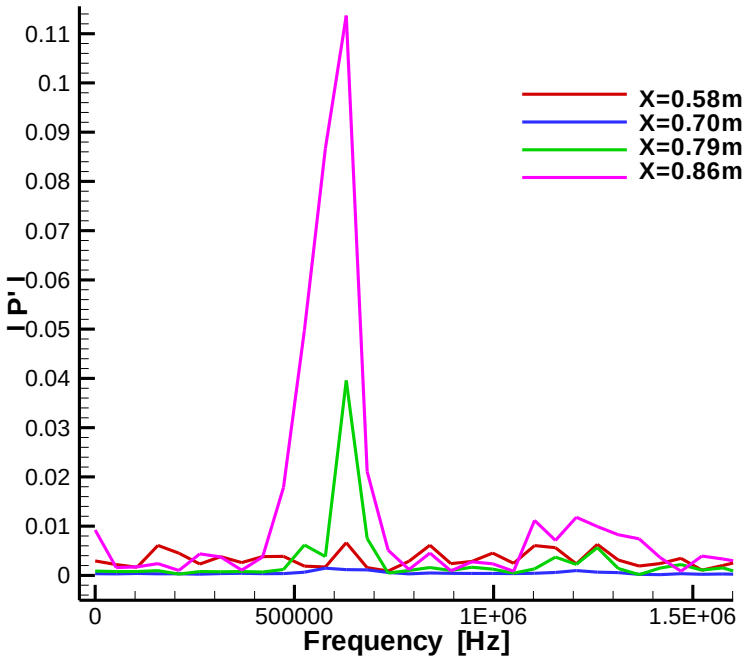

Fig. 12. Pressure amplitudes spectrum for spanwise wave number k=930

If looking at the range of unstable frequency, the growing waves at all the spanwise wave numbers are essentially in the same frequency range which falls inside the second mode instability frequency range. According to

the breakdown theory, this wave mode analysis indicated that the flow was undergoing the so-called fundamental breakdown process, which is commonly observed in incompressible flow transition.

V. Preliminary Result of TAMU MACH 6 Case

A. Mean Flow Calculation

The mean flow result is obtained using the cone geometry specified by TAMU Mach 6 quiet tunnel team. The cone nose radius is 0.125 inch. The cone is straight for the first half from the nose and flared for the second half. This design is adapted purposely to shorten the transition process. A clear compression effect in the flared section is observed from the pressure contour (Fig. 13).

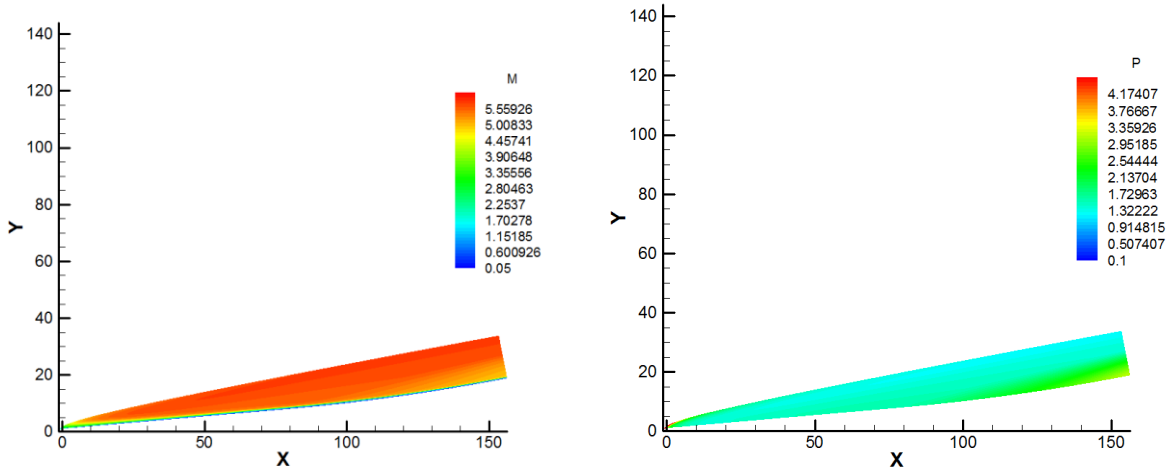

Fig. 13. Mach number contour and pressure contour for the cone with 0.125 inch nose bluntness.

B. Linear Receptivity Simulation

As the second step of current numerical study, the linear receptivity simulation that captures the mechanism of free stream disturbance entering the bow shock and interacting with boundary layer is conducted. We only consider using one type of disturbance at a time to make the analysis easier. In this case, only the fast acoustic waves are imposed to the freestream flow. Fig. 14 and Fig. 15 show the snapshots of pressure contour of the receptivity simulation at the nose region and the region right after it respectively. At the nose region, the freestream acoustic pulse passed the bow shock and hit the cone surface then reflected. As the wave reflected back from shock and nit the cone surface again, the wave amplitude dropped quickly. During this process, no boundary layer waves were excited. However, when the wave kept propagating onto the straight cone portion, the boundary layer mode started to emerge. The amplitude of boundary layer waves sustained at the same order of magnitude as it moved further downstream.

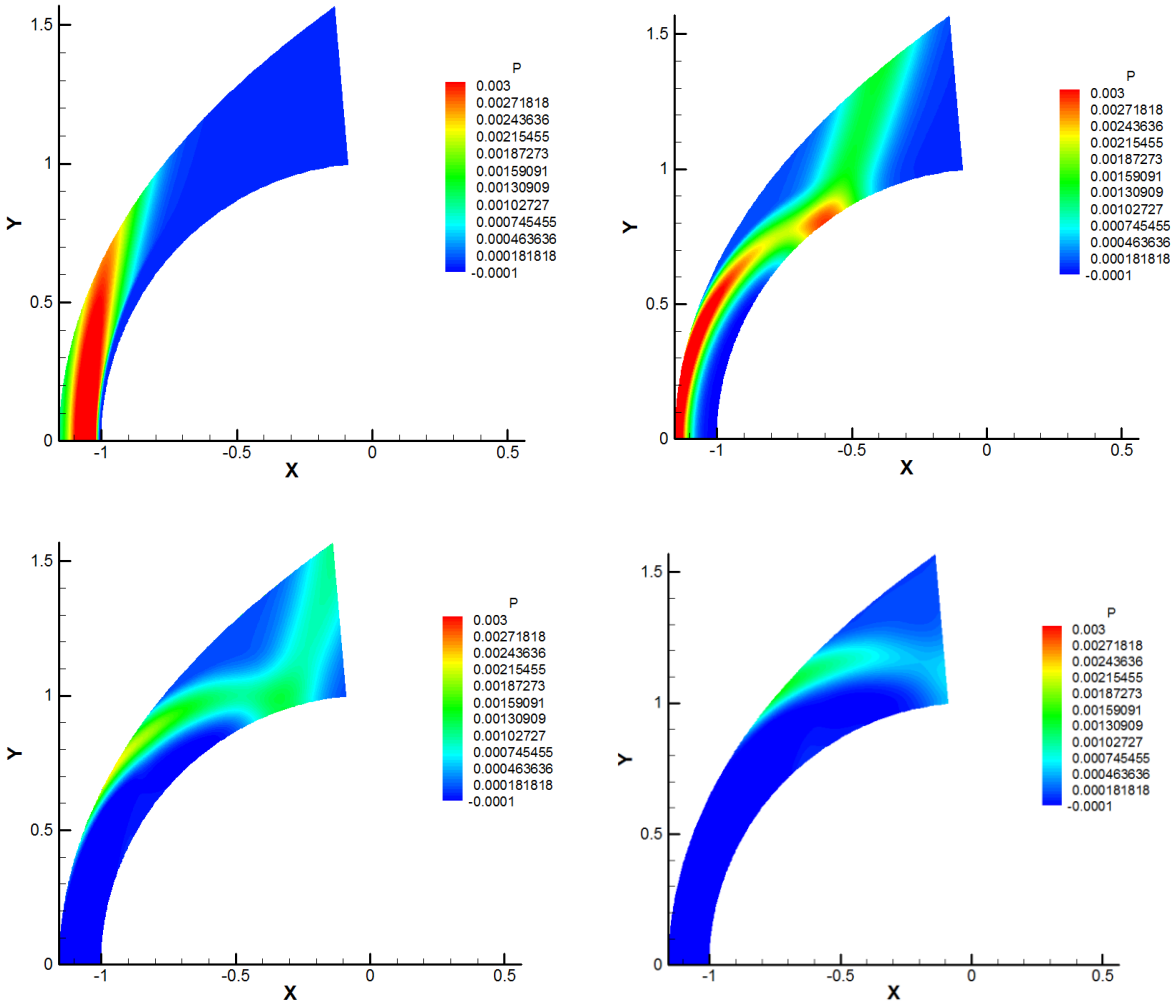

Fig. 14. Snapshots of pressure disturbance contour at the nose region (zone1) .

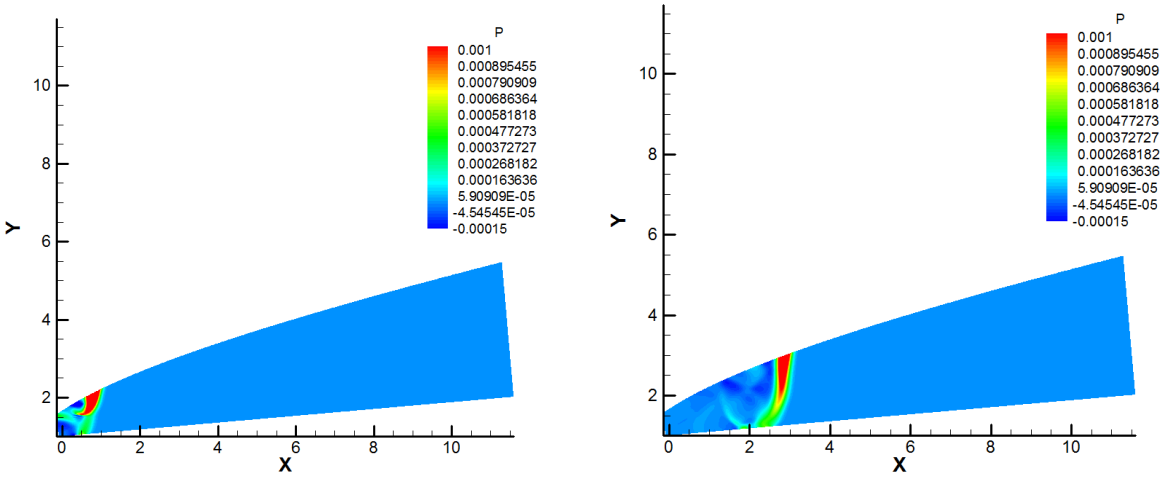

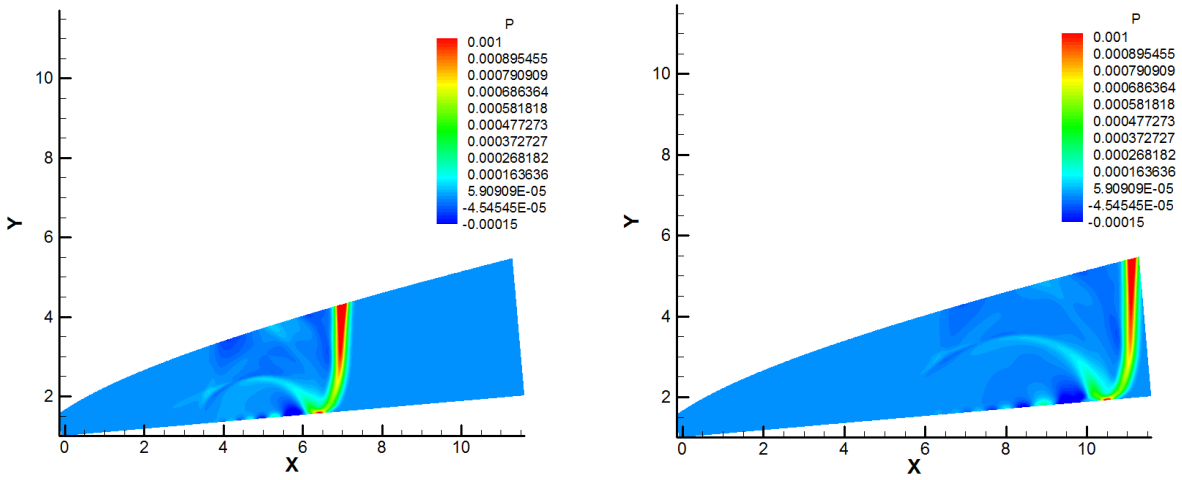

Fig. 15. Snap shot of pressure disturbance contour at the region right after nose (zone2).

From frequency spectrum, we can observe the evolution of waves as they propagate downstream. As shown in Fig. 16, the disturbance wave amplitudes decay quickly in the nose region after passing through the bow shock. At the region after the nose, as shown on Fig. 17 and Fig. 18, the wave spectrum kept oscillating while remained at comparable level. This spatial fluctuation can be explained by the reflecting acoustic waves bouncing between the shock and cone surface. This feature is unique to the acoustic dominated freesteam wave receptivity, which cannot be captured by other forcing introduction methods.

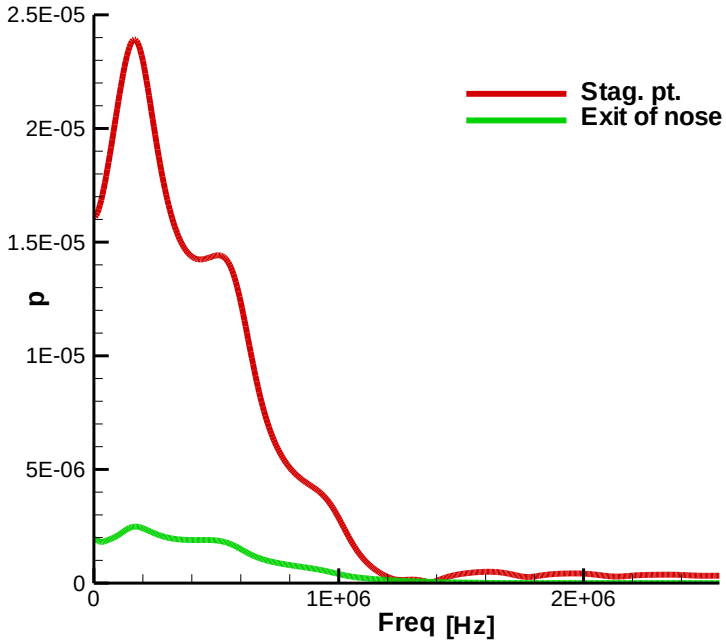

Fig. 16. Pressure Disturbances spectrum on the surface at stagnation point and exit of nose region.

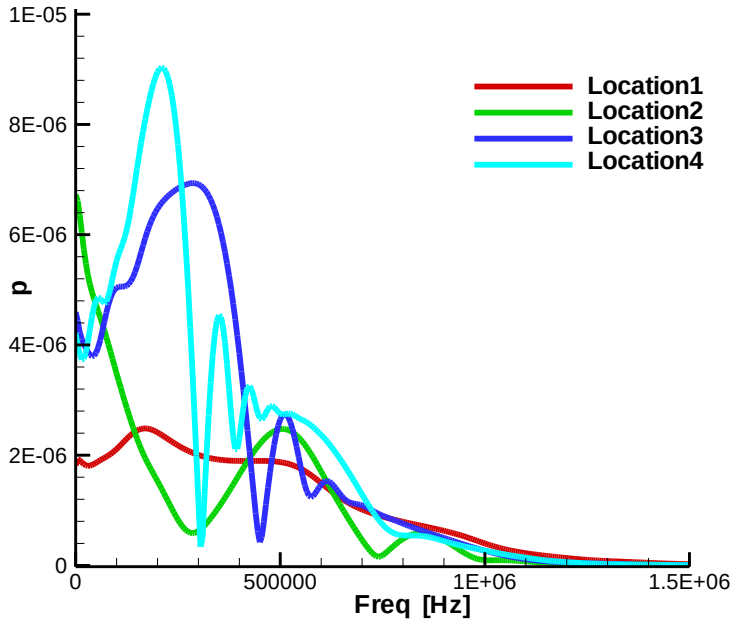

Fig. 17. Pressure Disturbances spectrum along the surface at equal-distant location for zone2.

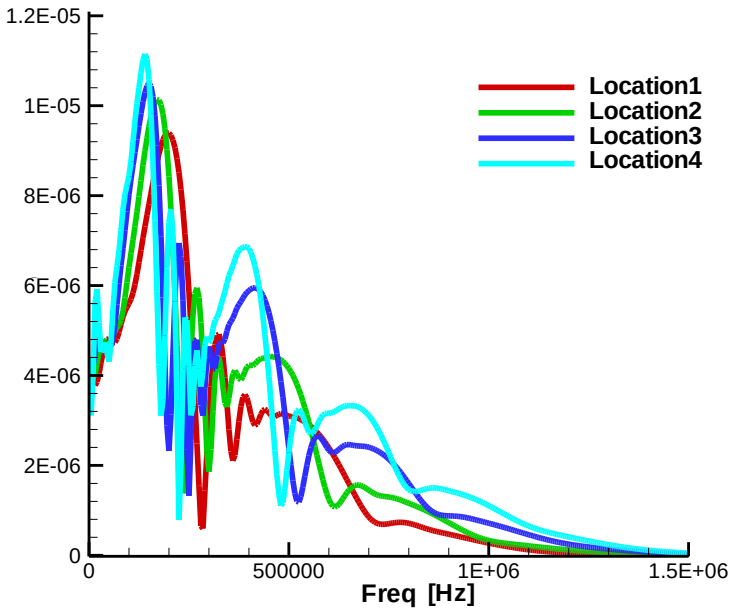

Fig. 18. Pressure Disturbances spectrum along the surface at equal-distant location for zone3.

The freestream receptivity simulation is still ongoing. We will carry it all the way until the instability waves appear. Then we will conduct the three dimensional nonlinear breakdown simulation the same way as shown for the Mach 5.5 test case. The advantage of using disturbance pulse with a continue frequency spectrum is to capture the

potential interaction between waves at different frequencies during the breakdown stage, which help better understand the linkage between freestream receptivity process and breakdown in transition.

VI. Summary and Future Work

The current numerical simulation study is still ongoing. In this paper, we demonstrated the feasibility of our new approach in investigation of hypersonic boundary layer transition induced by freestream waves. Also, some early works on the TAMU Mach 6 study case are presented. We are near in completion of the linear receptivity portion of the simulation. The subsequent 3-D nonlinear simulation will be carried out after we validate our receptivity simulation by comparing with either the theoretical analysis (i.e., LST study) or the experimental data from TAMU Mach 6 tunnel experiment team. The ultimate goal is to develop a robust numerical scheme to carry out hypersonic boundary layer flow simulation to the non-linear breakdown stage and provide a reliable tool for transition study.

Acknowledgments

This work was sponsored by AFOSR/NASA National Center of Hypersonic Research in Laminar-Turbulent transition and by the Air Force Office of Scientific Research, USAF, and Under Grant No.FA9550-07-1-0414, monitored by Dr. John Schmisseur. The views and conclusions contained herein are those of authors and should not be interpreted as necessarily representing the official policies or endorsement either expressed or implied, of the Air Force Office and Scientific research or U.S Government.

References

1. Kimmel, R.L., *Aspects of Hypersonic Boundary-Layer Transition Control.* 41st Aerospace Sciences Meeting and Exhibit, 2003. **AIAA paper 2003-0772**: p. 1-21.
2. Saric, W.S., Reed, H. L., and Kerschen, E. J., *Boundary-Layer Receptivity to Freestream Disturbances.* Annual Review of Fluid Mechanics, 2002. **34**: p. 291-319.
3. Zhong, X., *Additive Semi-Implicit Runge-Kutta Schemes for Computing High-Speed Nonequilibrium Reactive Flows.* Journal of Computational Physics, 1996. **128**: p. 19-31.
4. Zhong, X., *High-Order Finite-Difference Schemes for Numerical Simulation of Hypersonic Boundary-Layer Transition.* Journal of Computational Physics, 1998. **144**: p. 662-709.
5. Zhong, X., and Tatineni, M., *High-Order Non-Uniform Grid Schemes for Numerical Simulation of Hypersonic Boundary-Layer Stability and Transition.* Journal of Computational Physics, 2003. **190**(2): p. 419-458.
6. Zhong, X. *A New High-Order Immersed Interface Method for Multi-Phase Flow Simulation*. in *AIAA paper 2006-1294*. 2006.
7. Ma, Y., and Zhong, X., *Receptivity of a Supersonic Boundary Layer over a Flat Plate. Part 1: Wave Structures and Interactions.* Journal of Fluid Mechanics, 2003. **488**: p. 31-78.
8. Ma, Y., and Zhong, X., *Receptivity of a Supersonic Boundary Layer over a Flat plate. Part 2: Receptivity to Freestream Sound.* Journal of Fluid Mechanics, 2003. **488**: p. 79-121.
9. Ma, Y., and Zhong, X., *Receptivity to Freestream Disturbances of a Mach 10 Nonequilibium Reacting Oxygen Flow over a Flat Plate.* 2004. **AIAA 2004-0256**.
10. Ma, Y., and Zhong, X., *Receptivity of a Supersonic Boundary Layer over a Flat Plate. Part 3: Effects of Different Types of Free-Stream Disturbances.* Journal of Fluid Mechanics, 2005. **532**: p. 63-109.
11. Zhong, X., *Direct Numerical Simulation of Hypersonic Boundary-Layer Transition Over Blunt Leading Edges, Part II: Receptivity to Sound (Invited).* 1997. **AIAA Paper 97-0756**.
12. Zhong, X., *DNS of Boundary-Layer Receptivity to Freestream Sound for Hypersonic Flows over Blunt Elliptical Cones.* Laminar-Turbulent Transition, editors: H.F. Fasel and W.S. Saric, 1999: p. 445-450.
13. Zhong, X., *Leading-Edge Receptivity to Free Stream Disturbance Waves for Hypersonic Flow over a Parabola.* Journal of Fluid Mechanics, 2001. **441**: p. 315-367.
14. Zhong, X., *Receptivity of Mach 6 Flow Over a Flared Cone to Freestream Disturbance.* 2004. **AIAA 2004-0253**.
15. Zhong, X., and Ma, Y., *Boundary-layer receptivity of Mach 7.99 Flow over a blunt cone to free-stream acoustic waves.* Journal of Fluid Mechanics, 2005. **556**: p. 55-103.

16. Pruett, C.D., Zang, T. A., Chang, C. L., and Carpenter, M. H., *Spatial Direct Numerical Simulation of High-Speed Boundary-Layer Flows, Part I: Algorithmic Considerations and Validation.* Theoretical and Computational Fluid Dynamics, 1995. **7**: p. 49-76.
17. Pruett, C.D.a.C., C. L., *Spatial direct numerical simulation of high-speed boundary-layer flows Part II: Transition on a cone in Mach 8 flow* Theoretical and Computational Fluid Dynamics, 1995. **7**: p. 397-424.
18. Erlebacher, G., Hussaini, M. Y., *Numerical Experiments in Supersonic Boundary-Layer Stability.* Physics of Fluids A, 1990. **2**(1): p. 94-104.
19. Erlebacher, G.a.H., M. Y., *Stability and Transition in Supersonic Boundary Layers.* AIAA Paper 1987-1416, 1987: p. 1-12.
20. Thumm, A., Wolz, W., and Fasel, H. *Numerical simulation of spatially growing three-dimensional disturbance waves in compressible boundary layers*. in *Laminar-Turbulent Transition. IUTAM Symposium*. 1990. Toulouse, France, 1989 Springer-Verlag, Berlin.
21. Fasel, H., Thumm, A., and Bestek, H. *Direct numerical simulation of transition in supersonic boundary layers: oblique breakdown*. in *Fluids Engineering Conference, Transitional and Turbulent Compressible Flows*. 1993. Washington, DC, June 20–24, 1993: ASME, New York.
22. Chang, C.-L.a.M., M. R., *Oblique-mode breakdown and secondary instability in supersonic boundary layers.* Journal of Fluid Mechanics, 1994. **273**: p. 323-360.
23. Sandham, N.D., Adams, N. A., Kleiser, L., *Direct simulation of breakdown to turbulence following oblique instability waves in a supersonic boundary layer.* Applied Scientific Research, 1995. **54**: p. 223-234.
24. Mayer, C.S.J., von Terzi, D. A., and Fasel, H. F., *DNS of Complete Transition to Turbulence Via Oblique Breakdown at Mach 3.* AIAA paper 2008-4398, 2008: p. 1-21.
25. Laible, A., Mayer, C., and Fasel, H., *Numerical Investigation of Supersonic Transition for a Circular Cone at Mach 3.5*. AIAA paper 2008-4397 2008: p. 1-24.
26. Husmeier, F., Fasel, H. F., *Numerical Investigations of Hypersonic Boundary Layer Transition for Circular Cones.* AIAA paper 2007-3843, 2007: p. 1-17.
27. Stetson, K.F., Thompson, E. R., Donaldson, J. C., and Siler, L. G., *Laminar Boundary Layer Stability Experiments on a Cone at Mach 8, Part 1: Sharp Cone.* 1983. **AIAA Paper 83-1761**.
28. Stetson, K.F., Thompson, E. R., Donaldson, J. C., and Siler, L. G., *Laminar Boundary Layer Stability Experiments on a Cone at Mach 8, Part 2: Blunt Cone.* 1984. **AIAA paper 84-0006**.
29. Pruett, C.D.a.C., C. L., *Direct Numerical Simulation of Hypersonic Boundary-Layer Flow on a Flared Cone* Theoretical and Computational Fluid Dynamics, 1998. **11**: p. 49-67.
30. Rai, M.a.M., P., *Direct numerical simulation of transition and turbulence in a spatially evolving boundary layer.* AIAA Paper 91-1607, 1991: p. 890-912.
31. ADAMS, N.A., KLEISER, L., *Subharmonic transition to turbulence in a flat-plate boundary layer at Mach number 4.5*. Journal of Fluid Mechanics, 1996. **317**: p. 301-335.
32. Spalart, P.R., and Yang, K.-S., *Numerical study of ribbon-induced transition in Blasius flow.* Journal of Fluid Mechanics, 1987. **178**: p. 345-365.
33. Fedorov, A.V., and Khokhlov, A. P., *Prehistory of Instability in a Hypersonic Boundary Layer.* Theoretical and Computational Fluid Dynamics, 2001. **14**: p. 359-375.
34. Fedorov, A.V. *Receptivity of High Speed Boundary Layer to Acoustic Disturbances*. in *32nd AIAA Fluid Dynamics Conference*. 2002. St. Louis, MO.
35. Fedorov, A.V., and Khokhlov, A. P., *Receptivity of Hypersonic Boundary Layer to Wall Disturbances.* Theoretical and Computational Fluid Dynamics, 2002. **15**: p. 231-254.
36. Fedorov, A.V. *Receptivity of Hypersonic Boundary Layer to Acoustic Disturbances Scattered by Surface Roughness*. in *33rd AIAA Fluid Dynamics Conference*. 2003. Orlando, FL.
37. Tumin, A., Wang, X., and Zhong, X. *Direct Numerical Simulation and the Theory of Receptivity in a Hypersonic Boundary Layer* 2006.
38. Tumin, A. *Receptivity of Compressible Boundary Layers to Three-Dimensional Wall Perturbations*. 2006.
39. Egorov, I.V., Fedorov, A. V., and Soudakov, V. G. , *Direct Numerical Simulation of Unstable Disturbances in Supersonic Boundary Layer.* AIAA paper 2004-0588, 2004: p. 1-11.
40. Fedorov, A., and Tumin, A., *Initial-Value Problem for Hypersonic Boundary Layer* 2001. **AIAA Paper 2001-2781**.
41. Stetson, K.F., Rushton, G. H., *Shock Tunnel Investigation of Boundary-Layer Transition at M = 5.5.* AIAA JOURNAL, 1967. **5(5)**: p. 899-906.
42. Zhong, X., Lei, J., *Numericla Simulation of Nose Bluntness Effects on Hypersonic Boundary Layer Receptivity tp Freestream Disturbances.* 2011. **AIAA paper 2011-3079**.
43. Lei, J., Zhong, X., *Linear Stability Analysis of Nose Bluntness Effects on Hypersonic Boundary Layer Transition* Journal of Spacecraft and Rockets 0022-4650, 2011. **49**(1): p. 24-37.